Small Molecule Probe Diffusion in Thin Polymer Films Near the Glass Transition: A Novel Approach Using Fluorescence Nonradiative Energy Transfer[1]

Denise D. Deppe,[†] Ali Dhinojwala,[‡] and John M. Torkelson*[,†,‡]

Departments of Materials Science and Engineering and of Chemical Engineering, Northwestern University, Evanston, Illinois 60208

Received January 9, 1996; Revised Manuscript Received March 18, 1996[⊗]

ABSTRACT: A novel experimental approach involving fluorescence nonradiative energy transfer (NRET) is employed to study the Fickian diffusion of small molecules in rubbery polymer films near the glass transition. A theoretical formalism has been developed which directly relates the small molecule translational diffusion coefficient, D, to changes in the energy transfer efficiency, E. Values of D as low as 5×10^{-16} cm^2/s have been measured. In this approach, two thin polymer films are sandwiched together, one labeled with either NRET donor or acceptor chromophores and the second doped with the complementary chromophore. Upon annealing for a time t, dopant chromophore diffusion occurs in which E is proportional to $(Dt)^{1/2}/w$, where w is the donor film thickness. Values of D for pyrene, *N*-(2-hydroxyethyl)-*N*-ethyl-4-(tricyanovinyl)aniline (TC1), bis(phenylethynylanthracene) (BPEA), and decacyclene in poly(isobutyl methacrylate) (PiBMA) and for BPEA in poly(ethyl methacrylate) (PEMA) have been measured over temperatures ranging from ca. T_g to T_g + 20 °C. Among these chromophores, significant differences in both the magnitude and temperature dependence of D were observed and are attributed to differences in molecule size, shape, and flexibility. Two anomalous effects are observed from a comparison of translational diffusion and rotational reorientation dynamics of TC1 in PiBMA near T_g. The first is an apparent enhancement in translational diffusion relative to rotational reorientation dynamics, with the average translational displacement of a chromophore during an average rotational relaxation time, $\langle\tau_{rot}\rangle$, being a couple orders of magnitude larger than the length of the molecule. This behavior may be explained by significant local-scale heterogeneity in the polymer, i.e., the broad distribution of polymer α-relaxation times. The second regards the different temperature dependencies of $\langle\tau_{rot}\rangle$ and D near T_g. This may be explained qualitatively by a strong temperature dependence of the breadth of the distribution of α-relaxation times, an effect known to be present in the TC1−PiBMA system employed in this comparison as well as a variety of other polymer systems near T_g.

Introduction

There has been significant study recently concerning the diffusion of small molecules, with sizes larger than that of benzene but not polymeric, in bulk polymeric matrices. Technologically, this work has been driven by an interest in understanding diffusion-controlled phenomena such as those found in controlled drug release, coatings, and thermal printing applications. Scientifically, there is interest in understanding how small molecule motions, including rotational reorientation[2] and translational diffusion,[3] may be coupled to or decoupled from various polymer relaxation processes, such as the α-relaxation associated with cooperative segmental motions occurring near the glass transition temperature, T_g. Numerous techniques, including fluorescence quenching,[4,5] fluorescence recovery after photobleaching,[6,7] UV/vis and infrared spectroscopy,[8−10] mass uptake,[11,12] charge transfer techniques,[13] and capillary column inverse gas chromatography,[14,15] have been employed to measure translational small molecule diffusion coefficients on the order of 10^{-10} cm^2/s. To date, two techniques reported in the literature, forced Rayleigh scattering (FRS)[3,16−19] and holographic recovery after photobleaching (HFRAP),[20] have been used to measure significantly lower diffusion coefficients, 10^{-12}−10^{-16} cm^2/s, for molecules exhibiting Fickian diffusion[21] and some degree of coupling to the polymer α-relaxation process near T_g.

Here we present a new, relatively simple, and inexpensive approach allowing measurement of small molecule translational diffusion coefficients of magnitude comparable to those measured by FRS and HFRAP. This technique, a modification of a method recently described for measuring polymer interdiffusion,[22] involves fluorescence nonradiative energy transfer (NRET), which occurs when an excited-state donor chromophore transfers its energy to an acceptor chromophore via Coulombic dipole−dipole interactions over distances of a few nanometers. The approach employs a "sandwich" of two thin polymer films, each of which may be of thickness varying from a fraction to tens of microns depending upon the magnitude of the diffusion coefficient. One film is lightly labeled with either NRET donor or acceptor chromophores, and the other is doped at low levels with the complementary chromophore. Donor fluorescence from this "sandwich" is measured as a function of annealing time and temperature.

Given the many hundreds of well-known and characterized NRET donor−acceptor pairs available,[23] this approach affords the possibility of determining in detail how small molecule size, shape, and flexibility affect coupling of translational diffusion to polymer relaxations. Furthermore, this NRET approach allows for simple comparison of the temperature dependence of rotational reorientation dynamics[2] with that of translational diffusion for a number of chromophores which exhibit both fluorescence and second-order nonlinear optical properties in polymer films. An example will demonstrate that, for the chromophore/polymer pair studied, translational diffusion has an apparently weaker temperature dependence than rotational reorientation,

* To whom correspondence should be addressed.
† Department of Materials Science and Engineering.
‡ Department of Chemical Engineering.
⊗ Abstract published in *Advance ACS Abstracts,* May 1, 1996.

S0024-9297(96)00024-1 CCC: $12.00

which exhibits a temperature dependence equivalent to that of the α-relaxation. Implications of these studies for assessing the heterogeneous nature of amorphous polymers will be given.

Fluorescence NRET and Its Application to Small Molecule Diffusion within Polymer Matrices

Fluorescence NRET occurs when an excited donor chromophore transfers its excited-state energy to an acceptor chromophore via Coulombic dipole−dipole interactions over distances greater than several times the sum of the van der Waals radii of the donor−acceptor pair. In this study, NRET has been utilized via a simple geometry involving a "sandwich" of two thin polymer films. A film of polymer which is very lightly chemically labeled with either donor or acceptor chromophores is layered on top of a polymer film doped with a very small amount of the complementary chromophore. Initially, the chromophores lie on opposite sides of the interface, and little donor−acceptor interaction occurs. As polymer self-diffusion coefficients are many orders of magnitude lower than those of small molecules,[3,24] the polymer is considered to be stationary, while the dopant chromophores diffuse through it according to Fick's law. (The assumption of Fickian diffusion will be demonstrated to be correct based on the annealing time dependence of energy transfer efficiency.) Upon heating to a temperature near T_g, the free dopant chromophores diffuse into the chromophore-labeled polymer, the number of donor and acceptor chromophores in close proximity increases, and subsequently the probability for NRET increases. Experimentally, decreases in both the steady-state donor fluorescence intensity, I_D, and the average donor fluorescence lifetime, τ, are observed. The sample is illuminated by light of a wavelength preferentially absorbed by the donor, and decreases in I_D and τ are monitored.

Using this thin film geometry, we develop a general quantitative formalism to interpret measurements of both transient donor intensity decay and steady-state fluorescence in terms of small molecule diffusion. This approach is a modification of a method recently described for measuring polymer−polymer interdiffusion.[22] Two cases are considered as follows: (a) diffusion of dopant donor molecules into acceptor-labeled polymer and (b) diffusion of dopant acceptor molecules into donor-labeled polymer. These cases apply for polymer matrices both above and below T_g, and the labeled polymer is assumed to diffuse infinitesimally within the time frame that the dopant molecules diffuse, due to the orders of magnitude difference between small molecule and polymer diffusion coefficients.[3,24] In case a, donor diffusion coefficients are measured, and samples consist of an acceptor-labeled polymer film layered on top of a polymer film doped with donor molecules, as illustrated in Figure 1. Since the acceptor molecules remain essentially fixed in position during the experimental time frame, the acceptor concentration profile is given by

$$C_A(z,t) = \begin{cases} 0 & \text{for } -w < z < 0 \\ C_{AO} & \text{for } 0 < z < x \end{cases} \quad \text{for all diffusion times, } t \quad (1)$$

where w is the donor layer thickness and x is the acceptor layer thickness, and $w \leq x$. Assuming that the

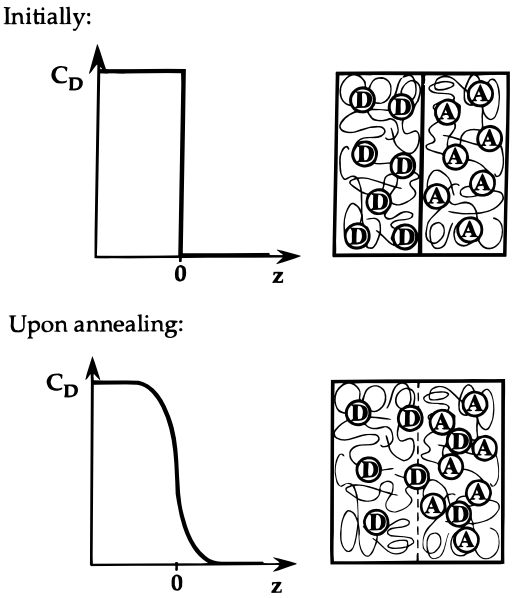

Figure 1. Sample geometry and donor chromophore concentration profile for case a, in which diffusion of the dopant donor occurs and the acceptor, chemically attached to the matrix polymer, remains essentially immobile.

diffusivity, D, of the free dopant chromophores (in this case the donor) is independent of concentration, the donor concentration profile can be determined using Fick's second law:[25,26]

$$\frac{\partial C_D(z,t)}{\partial t} = D\frac{\partial^2 C_D(z,t)}{\partial z^2} \quad (2)$$

Using the initial conditions that, at $t = 0$, $C_D(z,t) = C_{DO}$ for $-w < z < 0$ and $C_D(z,t) = 0$ for $0 < z < x$, for diffusion times $t \leq w^2/(16D)$, C_D is given by[26]

$$C_D(z,t) = \frac{C_{DO}}{2}\left(1 - \mathrm{erf}\left(\frac{z}{2\sqrt{Dt}}\right)\right) \quad (3)$$

This donor concentration gradient in the interfacial region may be combined with the relation proposed by Förster for the donor fluorescence intensity decay in the presence of acceptor chromophores[27,28] and integrated over the entire thickness of the layered sample:

$$I_{DN}(\bar{t},t) = \frac{1}{w}\int_{-w}^{x} \frac{C_D(z,t)}{C_{DO}} \exp\left[-\left(\frac{\bar{t}}{\tau_D}\right) - 2\gamma\left(\frac{\bar{t}}{\tau_D}\right)^{1/2}\right] dz \quad (4)$$

This equation assumes that both donor-to-donor energy transfer and energy transfer across the interface before diffusion are negligible.[29,30] In eq 4, $\bar{t}$ refers to decay time, t refers to annealing or diffusion time, $I_{DN}(\bar{t},t)$ is the donor intensity decay profile normalized to a value of 1 at $\bar{t} = 0$, τ_D is the donor lifetime in the absence of acceptors, and $\gamma = C_A/A_O$, where C_A is given in molar units and A_O is defined as

$$A_O = \frac{3000}{2N_A R_o^3 \pi^{3/2}} \quad (5)$$

where N_A is Avogadro's number and R_o is the Förster radius in centimeters. Since the acceptor molecules in this case are considered to be immobile, γ remains constant throughout the diffusion process.

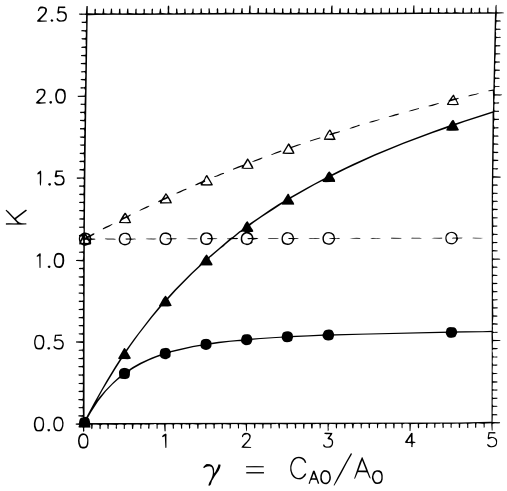

Figure 2. Parameter K from eqs 7, 8, 11, and 12 as a function of initial acceptor concentration, C_{AO}. Solid curve, filled circle: K_a from eq 7. Solid curve, filled triangle: K_b from eq 11. Dashed curve, open circle: K_{an} from eq 8. Dashed curve, open triangle: K_{bn} from eq 12. In general, solid curves and filled symbols correspond to fluorescence lifetime determinations of $E(t)$, whereas dashed curves and open symbols correspond to steady-state measurements of $E_N(t)$. Circles correspond to measurements of donor diffusion coefficients, and triangles correspond to acceptor diffusion coefficient measurements.

While eq 4 could, theoretically, be used to determine D through comparisons of experimental donor intensity decay profiles to simulations created using various values of D, a more straightforward approach involves determining the efficiency of energy transfer, $E(t)$:

$$E(t) = 1 - \frac{\int_0^\infty I_{DN}(\bar{t}/\tau_D,t)\, d(\bar{t}/\tau_D)}{\int_0^\infty I_{DN}(\bar{t}/\tau_D,0)\, d(\bar{t}/\tau_D)} = 1 - \frac{(\text{area under decay curve at time } t)}{(\text{area under decay curve at } t = 0)} \quad (6)$$

For the concentration profiles described by eqs 1 and 3, which apply for diffusion times $t \le w^2/(16D)$, this reduces to

$$E(t) = \left(\frac{\sqrt{Dt}}{w}\right)[\gamma \exp(\gamma^2)(1 - \text{erf}(\gamma))] = \left(\frac{\sqrt{Dt}}{w}\right)[K_a] \quad (7)$$

The parameter K_a, plotted as a function of C_{AO}/A_O in Figure 2, is constant for a given value of C_{AO}. E is therefore directly proportional to $\sqrt{t}$, and D at a particular temperature can be easily determined by measuring the donor fluorescence intensity decay of one unannealed sample and a number of samples annealed for various lengths of time at that temperature.

D can also be determined by steady-state measurements. The steady-state donor intensity can be related to the normalized efficiency of energy transfer:

$$E_N(t) = \frac{E(t)}{E(\infty)} = \frac{I_D(0) - I_D(t)}{I_D(0) - I_D(\infty)} = \left(\frac{\sqrt{Dt}}{w}\right)\left(\frac{2}{\sqrt{\pi}}\right) = \left(\frac{\sqrt{Dt}}{w}\right)[K_{an}] \quad (8)$$

where $I_D(0)$ and $I_D(\infty)$ are the initial donor fluorescence intensity and the donor intensity of a fully diffused sample, respectively. $I_D(0)$ is measured a few minutes after insertion into the sample holder in order to allow the quartz slide and polymer sandwich to come to thermal equilibrium. $I_D(\infty)$ is the fluorescence intensity of a sample consisting of an acceptor-labeled polymer film doped with donors at a concentration of $C_{DO}/2$ layered on top of a polymer film also doped with donors at a concentration of $C_{DO}/2$. Again, the parameter K_{an} is constant for a given value of C_{AO}. D is then determined from the slope of a plot of $E_N(t)$ vs $t^{1/2}$.

For case b, acceptor diffusion measurements, a donor-labeled polymer film is layered on top of an acceptor-doped film. The donors are now immobile, and D describes the Fickian diffusion of the acceptors through the polymer matrix. Concentration profiles are given by

$$C_D(z,t) = \begin{cases} C_{DO} & \text{for } -w < z < 0 \\ 0 & \text{for } 0 < z < x \end{cases} \text{ for all diffusion times, } t \quad (9)$$

$$C_A(z,t) = \frac{C_{AO}}{2}\left(1 + \text{erf}\left(\frac{z}{2\sqrt{Dt}}\right)\right) \quad (10)$$

Equation 10 is valid for diffusion times $t \le w^2/(16D)$, where w is again the thickness of the film containing the donor.[26] The acceptor concentration is changing, and γ, being a function of C_A, is now a function of diffusion time, t. Substituting eqs 9 and 10 into (4) and (6) yields

$$E(t) = \left(\frac{\sqrt{Dt}}{w}\right)[2\sqrt{\pi}\int_0^{w/(2\sqrt{Dt})} a \exp(a^2)(1 - \text{erf}(a))\, dy] = \left(\frac{\sqrt{Dt}}{w}\right)[K_b] \quad (11)$$

$$E_N(t) = \left(\frac{\sqrt{Dt}}{w}\right)\left[\frac{K_b}{\sqrt{\pi}(a_f)\exp(a_f^2)(1 - \text{erf}(a_f))}\right] = \left(\frac{\sqrt{Dt}}{w}\right)[K_{bn}] \quad (12)$$

where

$$a = \frac{C_{AO}}{2A_O}(1 - \text{erf}(y)),\ y = \frac{z}{2\sqrt{Dt}},\ \text{and}\ a_f = \frac{C_{AO}}{2A_O} \quad (13)$$

Again, the bracketed terms K_b and K_{nb} in eqs 11 and 12 are constants for a particular value of C_{AO}. These expressions are plotted as a function of C_{AO}/A_O in Figure 2.

Experimental Section

Pyrene (Aldrich) was used as the NRET donor, and decacyclene (Aldrich), 9,10-bis(phenylethynyl)anthracene (BPEA, Aldrich), and *N*-(2-hydroxyethyl)-*N*-ethyl-4-(tricyanovinyl)aniline (referred to as TC1, synthesized in this laboratory following the procedure outlined by McKusick et al.[31]) were used as NRET acceptors. Matrix polymers were poly(isobutyl methacrylate) (PiBMA) and poly(ethyl methacrylate) (PEMA). (Chemical structures of all materials are given in Figure 3.) Polymers were prepared by copolymerization of either pyrene-labeled monomer or TC1-labeled monomer with iBMA or EMA, as described previously,[2a] to produce chromophore-labeled polymer or by homopolymerization of only iBMA or EMA under the same conditions. T_g's of the polymers and copolymers (consisting of 99.88 mol % iBMA and 0.12 mol % pyrene-labeled monomer, 99.50 mol % iBMA and 0.50 mol % TC1-labeled monomer, or 99.88 mol % EMA and 0.12 mol % pyrene-labeled monomer, as determined by UV/vis spectroscopy) were

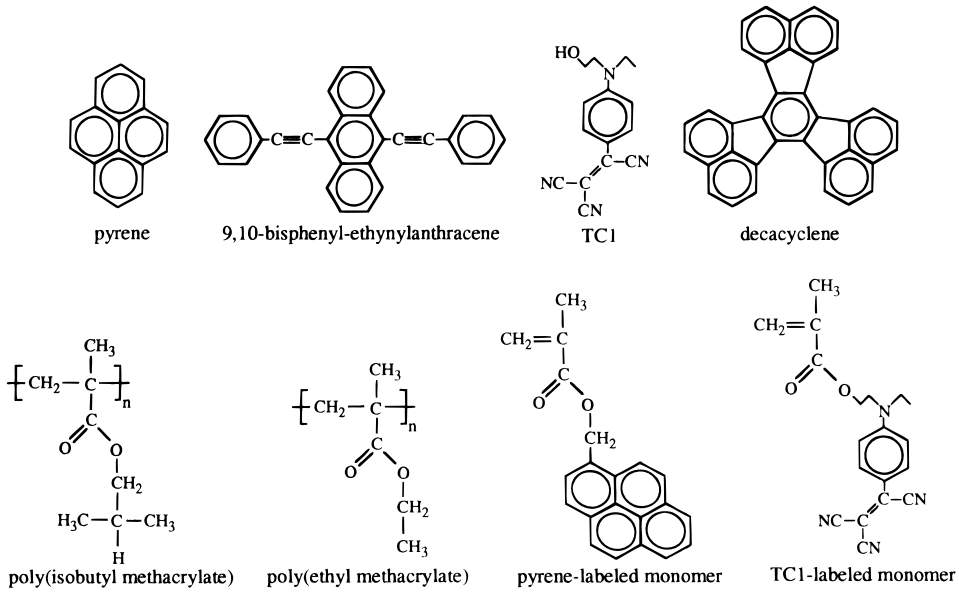

Figure 3. Chemical structures of the materials used in this study.

measured as the onset of the heat capacity change using a Perkin-Elmer DSC-7 instrument at a heating rate of 10 °C/min, with the PiBMA homopolymer and copolymers yielding identical T_g's of 64 °C and PEMA homopolymer and copolymers yielding identical T_g's of 75 °C. Polymers doped with 0.12 mol % pyrene or 0.50 mol % of one of the acceptor chromophores also yielded T_g's of 64 °C (PiBMA) and 75 °C (PEMA).[32] Förster radii (R_o, the donor−acceptor separation distance at which there is a 50% probability of energy transfer to acceptor[23]) of 3.7 nm for the pyrene/decacyclene donor−acceptor pair, 3.5 nm for pyrene/BPEA, and 3.0 nm for pyrene/TC1 were determined from the overlap in donor fluorescence and acceptor absorbance spectra.[23,33]

Films were spun cast onto quartz slides from chloroform solution and allowed to dry overnight at room temperature.[34] Film thicknesses, ranging from 0.32 to 15 μm, were characterized using a Tencor P10 profilometer. Layered samples were prepared by floating the chromophore-labeled polymer film off the slide onto the surface of a distilled water bath and placing this film on top of a slide coated with chromophore-doped polymer. Excess water was removed, and the polymer sandwich was allowed to dry for at least 24 h at room temperature and was then placed in a vacuum oven at room temperature for several hours to promote contact between layers.

Pyrene steady-state fluorescence intensity measurements were performed *in situ*, using a SPEX Fluorolog spectrophotometer equipped with a temperature-controlled sample cell.[35] All samples were excited at the pyrene absorbance maximum, 336 nm for pyrene dopant and 328 nm for pyrene-labeled polymer, and emission intensity was monitored at 372 nm for pyrene dopant and at 375 nm for pyrene-labeled polymer. Samples for lifetime measurements were annealed in an oven, and intensity decay profiles were collected at room temperature using a Photon Technologies International LS-100 spectrophotometer equipped with a time-correlated single-photon counting system. These profiles were fit to multiexponential decays using a linear least-squares method,[36] with the parameter χ^2 typically having values between 1.0 and 1.1. Areas under the decay curves were calculated using these multiexponential fits.

Results and Discussion

Bennett[37] demonstrated clearly in a study conducted over 30 years ago that the nonradiative energy transfer efficiency, E, between donor and acceptor chromophores doped randomly (i.e., homogeneously) into polymer films followed the prediction of Förster theory:[27,28,37,38]

$$E(\gamma) = \pi^{1/2}\gamma \exp(\gamma^2)(1 - \mathrm{erf}(\gamma)) \qquad (14)$$

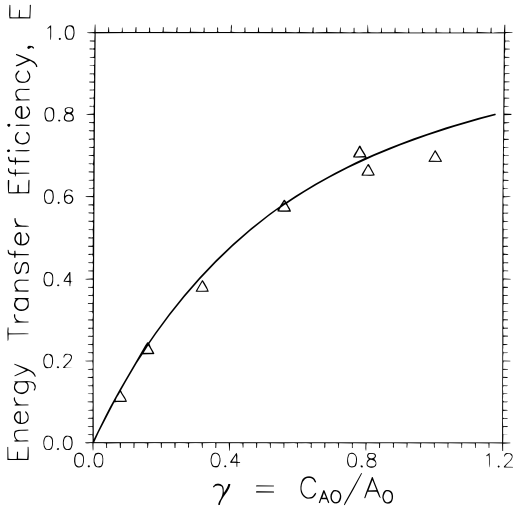

Figure 4. Experimental observation of energy transfer efficiency in BPEA-doped pyrene-labeled PiBMA films as a function of BPEA concentration (△), compared to Förster theory of energy transfer (solid curve).

in which $\gamma = C_{AO}/A_O$, as defined previously. In Figure 4 we provide examples of measurements such as these from the present study, specifically the energy transfer efficiency of homogeneous pyrene-labeled PiBMA films doped with varying concentrations of BPEA. Very good agreement between experimental observation of NRET and Förster theory is demonstrated. These simple measurements are important for two reasons: they serve as a check on the R_o value calculated for a donor/acceptor pair, and, because they demonstrate consistency with the Förster theory, they validate assumptions made in the development of the formalism described earlier for the determination of small molecule diffusion coefficients from NRET measurements.

An example of how the pyrene steady-state fluorescence intensity of a thin film "sandwich" sample may vary upon annealing is presented in Figure 5. *In situ* measurements are shown for a sandwich consisting of a TC1-labeled PiBMA film layered on top of a pyrene-doped PiBMA film and annealed at 70 °C, only a few degrees above the polymer T_g. Given the relatively high quantum yield of pyrene,[39] well-structured fluorescence spectra are obtained even at a low doping concentration

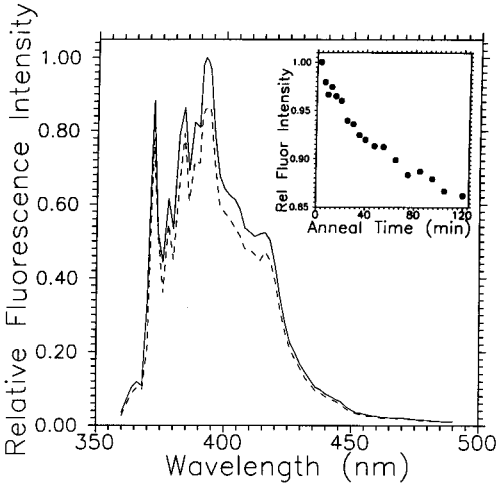

Figure 5. Steady-state fluorescence spectra of pyrene in layered pyrene-doped PiBMA/TC1-labeled PiBMA samples at 70 °C at annealing times of 3 min (solid curve) and 120 min (dashed curve). Inset: fluorescence emission intensity, monitored at 372 nm and normalized to an initial value of 1, as a function of *in situ* annealing time at 70 °C. $\lambda_{ex} = 336$ nm, $w = 1.6$ μm, and $K_{an} = 1.13$.

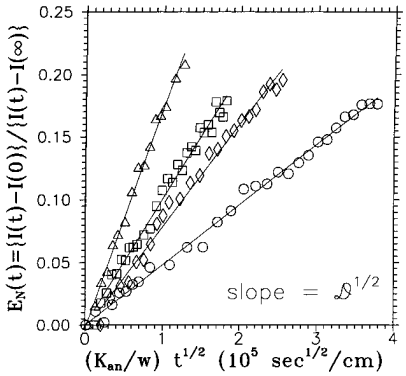

Figure 6. Normalized efficiency of energy transfer, E_N, as calculated from eq 8 at several temperatures for the layered pyrene-doped PiBMA/TC1-labeled PiBMA sample geometry: (○) $T = 65$ °C, (◇) $T = 70$ °C, (□) $T = 75$ °C, and (△) $T = 81$ °C.

of 0.12 mol % pyrene per polymer repeat unit in the thin pyrene-doped PiBMA films. The fractional decrease in intensity is uniform across the spectrum, resulting in a loss of signal of almost 15% after 2 h of annealing. The inset in Figure 5 shows the nonlinear, monotonic decrease in relative fluorescence intensity at 372 nm with annealing time.

Values of the normalized energy transfer efficiency, $E_N(t)$, for pyrene diffusion in PiBMA at several temperatures are calculated from such decreases in fluorescence intensity using eq 8 and are plotted as a function of $(K_{an}/w)t^{1/2}$ in Figure 6. The linearity of each plot is consistent with the rightmost term in eq 8, with the slope and thereby D increasing dramatically with temperature. Similar plots were obtained in the determination of diffusion coefficients of TC1, BPEA, and decacyclene in PiBMA (employing the pyrene-labeled copolymer of PiBMA in the sandwich) and BPEA in PEMA (employing the pyrene-labeled copolymer of PEMA) near T_g, indicating consistency with Fickian diffusion of these small molecules in PiBMA and PEMA.

Data of the type given in Figure 6 demonstrate that for thin film samples of appropriate thickness the determination of $E_N(t)$ using steady-state donor fluorescence intensity involves simple, straightforward *in situ* measurements which can yield diffusion coefficients

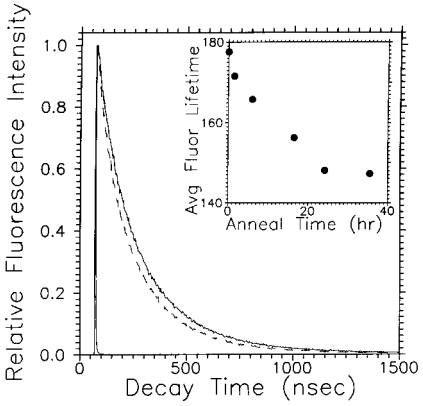

Figure 7. Pyrene intensity decay profiles of layered pyrene-labeled PiBMA/decacyclene-doped PiBMA film samples. Solid curve: unannealed sample. Dashed curve: after annealing for 35.5 h at 84 °C. Inset: average donor fluorescence lifetime as a function of annealing time at 84 °C. $\lambda_{ex} = 338$ nm, $\lambda_{em} = 374$ nm, $w = 3.2$ μm, and $K_b = 0.73$.

within a few hours or less of annealing time. However, there may be a limitation to the steady-state fluorescence technique in the case where significant photobleaching of one or both chromophores occurs during *in situ* illumination at elevated temperature. Such problems, which were not present in this study, may occur even when the sample is shuttered from illumination at all times except for a few seconds at each of the many intervals during the annealing at which an intensity measurement is taken. Therefore, a second method by which to calculate energy transfer efficiency is desirable. Because determination of NRET efficiency can be done using donor fluorescence intensity decays measured at room temperature after the thin film sandwich has been annealed in an oven, problems due to photobleaching during elevated temperature, *in situ* steady-state intensity measurements can be eliminated. Use of the fluorescence intensity decay technique may also prove beneficial when D values are exceedingly small ($\ll 10^{-16}$ cm^2/s), and the goal is to characterize diffusion in films thick enough so that no substantial deviation from bulk polymer behavior due to "ultrathin" character is discernible.[40] In these cases, the determination of a single diffusion coefficient by *in situ* steady-state intensity measurements could require the use of a fluorescence spectrometer for several weeks, leaving *ex situ* fluorescence intensity decay measurement the only practical method of determining the energy transfer efficiency.

Figure 7 shows donor fluorescence intensity decays from samples of pyrene-labeled PiBMA layered on top of decacyclene-doped PiBMA films, used in the determination of decacyclene diffusion coefficients. The average pyrene excited-state lifetime, τ, which is calculated as the area under the decay curve, of the unannealed sample was determined as 177.6 ns, a value which decreased to 147.3 ns upon annealing for 35.5 h. (The value of τ for the unannealed sample is comparable to the 169 ns decay time component attributed to pyrene monomer fluorescence which was measured by Jao et al.[41] in dilute solutions of ethylene-propylene copolymers labeled with single pyrene chromophores.) It should be mentioned that the fluorescence intensity decay profiles measured from these pyrene-labeled PiBMA films could not be described by single exponential decays;[42] for convenience, all of the decay profiles determined in this study were fit to multiexponential decays. However, it must be emphasized that the exact equation (or equa-

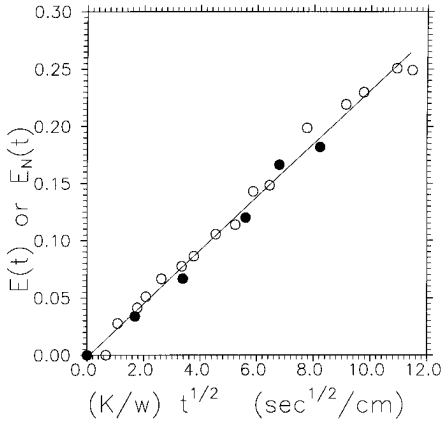

Figure 8. Efficiency of energy transfer as a function of annealing time at 84 °C in layered pyrene-labeled PiBMA/decacyclene-doped PiBMA: (●) E as determined from intensity decay measurements using eq 6 and (○) E_N as determined from steady-state measurements using eq 8. For lifetime measurements, λ_{ex} = 338 nm, λ_{em} = 374 nm, w = 3.2 μm, and K_b = 0.73; for steady-state measurements, λ_{ex} = 328 nm, λ_{em} = 375 nm, w = 0.43 μm, and K_{bn} = 1.2. Each data point represents the average of at least three measurements. Referring to eqs 11 and 12 in the text, it is readily seen that when E and E_N are plotted in this manner using the appropriate K_b and K_{bn} values, a straight line of slope = $D^{1/2}$ will result.

tions) to which the measured decay profile can be fit is not significant in the determination of energy transfer efficiency. Rather, the important experimental quantity is the area under each decay curve, yielding an average excited-state lifetime, and its value relative to that of the unannealed sample. The inset in Figure 7 shows the decrease of τ with anneal time.

Values of energy transfer efficiency, $E(t)$, were calculated from these τ values using eq 6 and are plotted in Figure 8. Also shown in Figure 8 are $E_N(t)$ values determined from *in situ* steady-state fluorescence measurements of pyrene-labeled PiBMA/decacyclene-doped PiBMA samples at 84 °C, as was done for the data plotted in Figure 6. A linear best fit to these data yields a slope of 2.3×10^{-7} cm/$s^{1/2}$, from which a D value of 5.4×10^{-14} cm^2/s is calculated. Data determined from the two techniques overlap perfectly, an indication that either $E_N(t)$, as measured by steady-state fluorescence intensity, or $E(t)$, as measured by donor fluorescence intensity decay, can be used to calculate D.

Figure 9 illustrates values of D for TC1, pyrene, BPEA, and decacyclene at several temperatures near and above T_g in PiBMA. D values as low as 5×10^{-16} cm^2/s can be determined within diffusion times of several hours, employing films 0.33 μm thick, demonstrating the ability of this approach to allow measurement of very low diffusion coefficients within relatively short times. Evident in Figure 9 is the significant difference in magnitude among diffusion coefficients for the four chromophores, with the highest D values observed for the relatively small and flexible TC1 chromophore and the lowest D values for rigid decacyclene, the largest chromophore. In addition, the temperature dependence appears to increase with increasing chromophore size, which could be interpreted as a qualitative indication that larger probes are coupled to the α-relaxation dynamics to a greater degree than are smaller diffusants. (An alternative explanation will be provided later.) Also shown in Figure 9 are diffusion data for BPEA in PEMA from this study and for 2,2′-bis(4,4-dimethylthiolan-3-one) (referred to as TTI) in PEMA from ref 3. When plotted relative to T_g, the

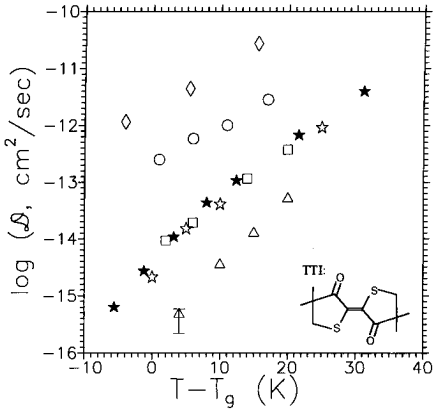

Figure 9. Temperature dependence of the translational diffusion coefficients of (◊) TC1, (○) pyrene, (□) BPEA, and (Δ) decacyclene in PiBMA, T_g = 64 °C, and (☆) BPEA in PEMA, T_g = 75 °C, as determined in this study, compared to the temperature dependence of the translational diffusion of (★) TTI in PEMA, T_g = 69 °C, as determined by Ehlich and Sillescu in ref 3. Typically, error is represented by the symbol size, with one exception, which is shown.

BPEA diffusion coefficients in PEMA and PiBMA overlap. (Using second-harmonic generation measurements, an overlapping temperature dependence of the rotational reorientation dynamics of nonlinear optical dyes, such as Disperse Red 1 and TC1, has also been observed in PiBMA and PEMA when data are shifted with respect to T_g. This has been attributed to a similar dependence of the α-relaxation processes or cooperative segmental dynamics in PiBMA and PEMA.[2c,43,44]) The BPEA data from this study also overlap Ehlich and Sillescu's TTI data,[3] demonstrating virtually the same temperature dependence and magnitude.

The diffusion data can be analyzed more quantitatively using a modification of the Williams−Landel−Ferry (WLF) relation,[45] which can be used to describe the temperature dependence of small molecule motions above the glass transition temperature:[3,46]

$$\log\left[\frac{D(T)}{D(T_g)}\right] = \frac{\xi C_{1g}(T - T_g)}{(C_{2g} + T - T_g)} \qquad (15)$$

in which C_{1g} and C_{2g} are the familiar WLF parameters and ξ is a coupling parameter, which will be discussed in detail later. The diffusion data for TTI (from ref 3) and BPEA (from this study) in PEMA were fit to eq 15, and the results are listed in Table 1. For each fit, C_{1g} and C_{2g} were held constant, while the values of ξ and D at T_g were varied. Two sets of WLF parameters for PEMA were used in the fits: C_{1g} = 15 and C_{2g} = 90 K, from ref 3, and C_{1g} = 14 and C_{2g} = 62 K, from ref 2a. Because Ehlich and Sillescu performed measurements over a much larger temperature range than was used here, their results were truncated to a 23 °C temperature range near T_g. For each set of WLF parameters used in Table 1, ξ values determined from the small temperature range fits to Ehlich and Sillescu's TTI data and from our BPEA data show excellent agreement, a quantitative verification of the overlap observed in Figure 9. However, a small difference is observed between ξ values determined using Ehlich and Sillescu's WLF parameters[3] when compared to the ξ values determined using the WLF parameters of Dhinojwala et al.[2a] To demonstrate that either set gives a good fit, the TTI and BPEA diffusion coefficients are plotted in Figure 10, along with WLF curves calculated using each

Table 1. Analysis of Small Molecule Diffusion in PEMA[67]

			using $C_{1g} = 15$, $C_{2g} = 90$ K[a]			using $C_{1g} = 14$, $C_{2g} = 62$ K[b]		
probe	matrix T_g, K	E_a, kJ/mol	ξ	$\log(D(T_g))$	$E_a/(E_a)_\alpha$	ξ	$\log(D(T_g))$	$E_a/(E_a)_\alpha$
TTI[c]	342		0.81[e]	−14.2[e]		0.75	−14.5	
TTI[d]	342	24_8	0.75	−14.4	0.73	0.62	−14.4	0.62
BPEA	348	25_3	0.75	−14.6	0.74	0.61	−14.6	0.64

[a] WLF parameters from ref 3. $(E_a)_\alpha = 34_2$ kJ/mol, from eq 16 at $T_g + 8$ °C. [b] WLF parameters from ref 2a. $(E_a)_\alpha = 39_7$ kJ/mol, from eq 16 at $T_g + 8$ °C. [c] Fit to data over the temperature range 341−431 K ($T_g - 1$ °C < T < $T_g + 89$ °C, overall T range). [d] Fit to data over the temperature range 341−364 K ($T_g - 1$ °C < T < $T_g + 22$ °C, low-T range). [e] Value determined in ref 3.

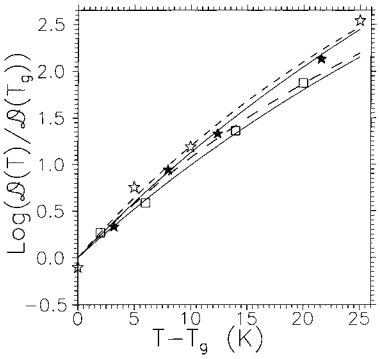

Figure 10. Comparison of the fits described by the different sets of Williams−Landel−Ferry (WLF) parameters used for data analysis. Translational diffusion coefficients of (□) BPEA in PiBMA, $T_g = 64$ °C, and (☆) BPEA in PEMA, $T_g = 75$ °C, from this study, and (★) TTI in PEMA, $T_g = 69$ °C, as determined by Ehlich and Sillescu in ref 3. PEMA data are fit using $C_{1g} = 15$, $C_{2g} = 90$ *K*, and $\xi = 0.75$ (upper solid curve) and $C_{1g} = 14$, $C_{2g} = 62$ K, and $\xi = 0.62$ (upper dashed curve). PiBMA data are fit using $C_{1g} = 15$, $C_{2g} = 90$ K, and $\xi = 0.66$ (lower solid curve) and $C_{1g} = 13$, $C_{2g} = 90$ K, and $\xi = 0.58$ (lower dashed curve). Refer to Tables 1 and 2 for the source of each set of WLF parameters.

set of parameters. Both curves appear to be acceptable representations of the data. Attempts were also made at fitting the data without constraining the values of C_{1g} and C_{2g}, but no dependable fit could be obtained due to the small temperature range used here. However, because this 16 °C temperature range is fairly narrow, data that would follow a WLF-type relation over a wider temperature range could be fit very well to a simple, apparent Arrhenius relation. From these fits, apparent activation energies, E_a, and effective coupling parameters, $E_a/(E_a)_\alpha$, were calculated and are listed in Table 1. $(E_a)_\alpha$ is considered to be the effective activation energy of the α-relaxation and is calculated at $T_g + 8$ °C, the middle of the temperature range, from the WLF parameters:[45]

$$(E_a)_\alpha(T) = \frac{2.303RC_{1g}C_{2g}T^2}{(C_{2g} + T - T_g)^2} \qquad (16)$$

in which R is the gas constant. For both sets of WLF parameters and for both TTI and BPEA, the ratio $E_a/(E_a)_\alpha$ calculated in this manner is in excellent agreement with the coupling parameter ξ determined from the constrained WLF fits.

A similar approach was used to compare the temperature dependencies of the TC1, pyrene, BPEA, and decacyclene diffusion coefficients to the α-relaxation dynamics in PiBMA, using the WLF parameters $C_{1g} = 13$ and $C_{2g} = 58$ K, determined from dielectric and second-harmonic generation measurements in PiBMA,[2a] and $C_{1g} = 15$ and $C_{2g} = 90$ K, determined in ref 3 for PEMA. The results are recorded in Table 2. Again it is observed that $E_a/(E_a)_\alpha$ ratios calculated from the apparent Arrhenius fits agree well with the coupling parameter ξ determined from the constrained WLF fits. In addition, both sets of WLF parameters give acceptable fits to the diffusion data, as shown in Figure 10 for BPEA. The sizes of the molecules, calculated as the molar volume at 0 K using the Sugden group contribution method as reviewed by Haward,[47] are also listed in Table 2. Among the rigid molecules, pyrene is the smallest, having a molar volume at 0 K of 151 cm^3/mol, and its translational diffusion exhibits only ca. 40% of the temperature dependence of the α-relaxation dynamics in PiBMA. BPEA, with a much larger molar volume at 0 K of 288 cm^3/mol, exhibits a greater temperature dependence, about 60% of the α-relaxation dynamics. The translational diffusion coefficient of decacyclene, which has a molar volume at 0 K of 314 cm^3/mol, exhibits the largest temperature dependence, ca. 80−90% of the α-relaxation dynamics. Increasing chromophore size results in a greater "apparent" degree of coupling to the polymer α-relaxation dynamics. An interesting result is obtained from analysis of the diffusion of TC1, which, with a molar volume of 201 cm^3/mol, is quite a bit larger than pyrene. TC1 can diffuse ca. 1 order of magnitude faster than pyrene, even though it is one-third larger in volume; this is apparently associated with the flexible side groups attached to the single ring of TC1, enhancing its mobility relative to that of the rigid pyrene molecule.

For all the systems studied here, values of the parameter ξ fit well within the bounds of 0 and 1 expected by Ehlich and Sillescu.[3,48] ξ can be interpreted on the basis of Vrentas−Duda free volume theory[49] as the ratio of the critical molecular volume of the solute jumping unit, v_s^*, to the critical molecular volume of the polymer matrix jumping unit, v^*; $\xi = v_s^*/v^*$. An implication of this result is that ξ values for different rigid solutes in the same matrix can be related by

$$\frac{\xi(\text{solute 1})}{\xi(\text{solute 2})} = \frac{\text{molar volume at 0 K of jumping unit (solute 1)}}{\text{molar volume at 0 K of jumping unit (solute 2)}} \qquad (17)$$

Interestingly, an equivalence apparently holds for the ratio ξ(pyrene)/ξ(decacyclene) in PiBMA, equal to 0.47, and a like ratio of overall molar volumes at 0 K (see values in Table 2), equal to 0.48. (This does not imply that the total volume of pyrene or decacyclene constitutes the "jump unit" size, merely that the jump unit sizes of pyrene and decacyclene comprise equivalent fractions of their overall volumes.) However, this relationship does not hold for comparisons involving either TC1 or BPEA, apparently due to the mobility around the single bonds in these chromophores, which is not present in the rigid pyrene and decacyclene molecules. The elongated shape of BPEA in comparison

Table 2. Analysis of Small Molecule Diffusion in PiBMA, T_g = 337 K

			using $C_{1g} = 13$, $C_{2g} = 58$ K[a]			using $C_{1g} = 15$, $C_{2g} = 90$ K[b]		
probe	size, cm^3/mol[c]	E_a, kJ/mol	ξ	log($D(T_g)$)	$E_a/(E_a)_\alpha$	ξ	log($D(T_g)$)	$E_a/(E_a)_\alpha$
TC1	201	15_8	0.37	−11.6	0.42	0.46	−11.7	0.46
pyrene	151	14_7	0.38	−12.7	0.40	0.45	−12.7	0.43
BPEA	288	21_2	0.56	−14.3	0.57	0.66	−14.3	0.62
decacyclene	314	29_4	0.81	−16.0	0.79	0.96	−15.9	0.86

[a] WLF parameters for PiBMA from ref 2a. $(E_a)_\alpha = 37_0$ kJ/mol, from eq 16 at $T_g + 8$ °C. [b] WLF parameters for PEMA from ref 3. $(E_a)_\alpha = 34_2$ kJ/mol, from eq 16 at $T_g + 8$ °C. [c] Molar volumes at 0 K calculated using the group contribution method developed by Sugden, as reviewed by Haward.[47]

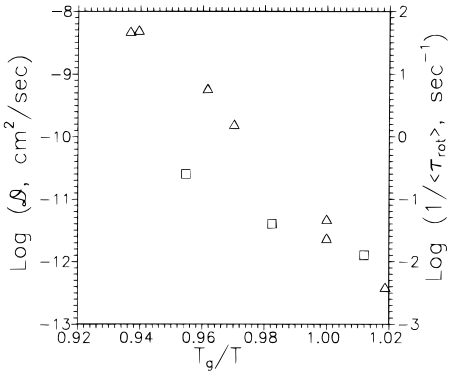

Figure 11. TC1 dynamics in PiBMA: comparison between the temperature dependencies of the (□) translational diffusion coefficient, D, and (△) average rotational reorientation relaxation times, $\langle\tau_{rot}\rangle$. ($\langle\tau_{rot}\rangle$ values taken from refs 43 and 44.)

to the disklike shape of pyrene and decacyclene may also be a factor. (Shape effects are not considered in the Vrentas−Duda interpretation.) The similar D and ξ values for BPEA and TTI in PEMA also do not scale with chromophore size, with the molar volume at 0 K of TTI calculated[47] as 185 cm^3/mol, roughly two-thirds that of BPEA. Due to anisotropic diffusion effects, the elongated shape of BPEA may contribute to a temperature dependence less than that expected for a molecule of similar size but with a smaller aspect ratio. Ehlich and Sillescu[3] have a more complex interpretation of $1 - \xi$ as a decoupling parameter, accounting for the decoupling of solute diffusion from the α-relaxation process of the matrix. A major implication of their interpretation is that the ratio $[1 - \xi(\text{solute 1})]/[1 - \xi(\text{solute 2})]$ is apparently independent of the matrix; comparisons of this type will be made in the near future using the NRET approaches outlined here.

Finally, a comparison of the temperature dependencies of the rotational reorientation dynamics and translational diffusion of TC1 in PiBMA is given in Figure 11. Second-harmonic generation studies of rotational reorientation dynamics have demonstrated apparently complete coupling of the rotational dynamics of TC1, as characterized by the equivalence of the temperature dependencies of the average rotational reorientation relaxation time, $\langle\tau_{rot}\rangle$, to that of the α-relaxation dynamics of PiBMA.[2a,43,44] Over the temperature range shown in Figure 11, the translational diffusion coefficient of TC1 is apparently much less temperature dependent than $\langle\tau_{rot}\rangle$. (An Arrhenius fit to the $\langle\tau_{rot}\rangle$ data in Figure 11 yields an activation energy of $E_a = 330$ kJ/mol, as compared with the value of 370 kJ/mol calculated from eq 16 at $T_g + 8$ °C using $C_{1g} = 13$ and $C_{2g} = 58$ K, determined from a WLF fit to the data.[2a] Using this value as $(E_a)_\alpha$ would yield slightly higher values of $E_a/(E_a)_\alpha$, but the essential trends discussed here would remain unchanged.) A simple interpretation would be that translational diffusion is less coupled than rotational reorientation to the polymer α-relaxation process. The same effect has been observed in studies of small molecule dynamics in low molecular weight glass formers;[50] similar behavior has also been reported in polymeric systems.[20,51,52]

An anomalous conclusion that may be reached from this comparison of the rotational and translational dynamics of chromophores in polymers at temperatures slightly above T_g is that apparently large-scale *average* translational motions can occur during one *average* rotational reorientational relaxation time of a probe molecule. For example, the mean-square displacement during the average reorientation time can be calculated as $\langle r^2\rangle = 6D\langle\tau_{rot}\rangle$. For TC1 in PiBMA at T_g, $D \approx 2 \times 10^{-12}$ cm^2/s and $\langle\tau_{rot}\rangle \approx 30$ s, yielding $\langle r^2\rangle \approx (200\text{ nm})^2$. In other words, the root-mean-square displacement during one average reorientation relaxation time is over 2 orders of magnitude greater than the length of the TC1 molecule, which is about 1 nm. At $T_g + 16$ °C, $D \approx 3 \times 10^{-11}$ cm^2/s and $\langle\tau_{rot}\rangle \approx 0.13$ s, yielding $\langle r^2\rangle \approx (50\text{ nm})^2$; at this temperature, the root-mean-square displacement is still more than 1 order of magnitude greater than the length of TC1. This anomalous effect, which indicates that, on average, a probe molecule can translate several orders of magnitude times its length during the average time required to undergo rotational reorientation near T_g, has been noted quantitatively in both low molecular weight and polymeric glass formers.[18,50]

In contrast to the possible interpretation that this anomaly results from the translational motions being less coupled than rotational reorientation to the α-relaxation dynamics, we believe that it results from the fact that the translational diffusion and rotational reorientation in fact reflect *different* portions of the distribution of α-relaxation times. This means that the translational diffusion coefficients measured here are averages which are dominated by the most mobile local regions in the polymer which have the largest individual D values and correspond to the shortest relaxation times ($D \sim 1/\tau_{rot,fast}$ as an oversimplification), meaning that the largest extent of translational motion will occur by molecules in environments with the shortest relaxation times. On the other hand, average rotational relaxation dynamics reflect the slow relaxing environments ($\langle\tau_{rot}\rangle \sim \tau_{rot,slow}$ as an oversimplification). The latter point is supported by the demonstration via second-harmonic generation studies[2a,43] that, other factors being constant, narrowing the distribution of reorientational relaxation times through the loss of the shortest time components, as by the use of extremely large chromophores, results in no change in $\langle\tau_{rot}\rangle$, within experimental error. In other words, for a very broad distribution, the average relaxation time, calculated as the area under a relaxation curve plotted on a linear time scale, will reflect the longer part of the distribution. Consequently, given that the relaxation distribution covers many orders of magnitude in time for the TC1−

PiBMA system, it is not necessary that any *single* TC1 chromophore translates many times its length during the time required to relax its orientation. Instead, in a system with a high degree of local heterogeneity or a broad distribution of relaxation times, $\langle\tau_{rot}\rangle$ does not reflect translational diffusion time scales, and such anomalous results will occur when calculations of translational displacement are based on average rotational relaxation times. Only in the case where local heterogeneity or the breadth in the distribution of local relaxation environments is significantly reduced, more nearly approximating that of a single relaxation time, would such a calculation be expected to yield a "reasonable" result where the root-mean-square displacement achieved during the average rotational relaxation time would be of the order of the length of the molecule. Thus, when the distribution of rotational relaxation times narrows, as in the case of much larger probes,[43,53] the apparent enhancement in average translational dynamics as compared with rotational dynamics is expected to be significantly reduced; studies of such effects are underway.

Many possible reasons have been postulated recently for the apparently weaker temperature dependence of D as compared with rotational dynamics in polymers near T_g.[3,20,50−52,54,55] Some of these can be related to the strikingly broad distribution of relaxation times near T_g, covering many orders of magnitude in time.[2,43,44,50,55−57] However, the fact that polymers have very significant, local-scale heterogeneity near T_g[58,59] is not sufficient by itself to explain the different temperature dependencies of the translational and rotational dynamics of probe molecules. If the breadth of the distribution of relaxation times remains constant but is simply shifted to longer times as temperature is decreased, then the same temperature dependencies would be obtained for D and $\langle\tau_{rot}\rangle$ regardless of the fact that translational diffusion would appear to be enhanced with respect to rotational reorientation. A sufficient requirement for substantially different temperature dependencies is that the breadth of the distribution of relaxation times varies significantly over a relatively small range of temperature. These broad relaxation distributions cannot be described by a single relaxation time and are commonly fit to a stretched exponential expression, also known as the Kohlrausch−Williams−Watts equation. In this type of analysis, normalized relaxation decay data are fit to $\exp(-(t/\tau_r)^{\beta})$, where τ_r is a characteristic relaxation time and β is related to the breadth of the distribution. ($0 < \beta < 1$, where $\beta = 1$ corresponds to a single-exponential decay with a single relaxation time and $\beta = 0$ would correspond to an infinitely broad distribution of relaxation times.) In studies of TC1-doped PIBMA,[43,44] as well as a whole range of other probe−polymer systems investigated by second-harmonic generation studies[2c,43,60] (and α-relaxation dynamics measured using dielectric spectroscopy and dynamic light scattering[61]), it has been shown that the breadth of the distribution of relaxation times, and consequently the β parameter, can vary significantly with temperature. In these systems, β can approximately double in value, associated with a significant narrowing of the distribution of relaxation times, over less than a 50 °C increase in temperature from slightly below T_g to well into the rubbery state. (The impact on the temperature dependencies of D and $\langle\tau_{rot}\rangle$ by the significant narrowing of the distribution of relaxation times with small increases in temperature from T_g into the rubbery state will be discussed quantitatively in the near future.[60])

The fact that, for rigid chromophores, the temperature dependence of D increases with increasing size, more closely approximating that of the α-relaxation, may also be explained by changes in the breadth of the distribution of relaxation environments. Second-harmonic generation[43,53,62] and fluorescence bleaching[63] studies of probe rotational dynamics provide substantial evidence that when chromophores differ significantly in size, the shortest range of relaxation times can be truncated for the larger chromophores, resulting in narrower distributions of relaxation environments near T_g. When the distribution of relaxation times near T_g is already relatively narrow, decreases in the breadth of the distribution as a result of increasing the temperature will be less dramatic in comparison to a case in which the distribution is more broad. Consequently, the temperature dependencies of translational and rotational dynamics for a large probe will be more similar than those for a smaller molecule. (For decacyclene, the largest probe used in this study, the temperature dependence of translational motion is ca. 80−90% of that of rotational reorientation, which is expected to be equivalent to the temperature dependence of the α-relaxation. In contrast, for the probe pyrene, which has a molar volume at 0 K of ca. one-half that of decacyclene, the temperature dependence of translational motion is only about 40% of that of rotational reorientation.)

Studies are continuing in order to investigate these issues more fully, as well as to determine the effects of shape (with molecules of similar volume, anisotropic diffusion may yield higher D values for molecules which are long and narrow, as opposed to disk-shaped molecules; anisotropic effects may also alter the apparent rotational dynamics depending on which rotations are being measured) and flexibility (employing variations of the TC1 molecule) on the translational and rotational reorientation dynamics of small molecules in polymers near T_g. Related studies of the effects of size, shape, and flexibility on probe translational[64] diffusion in polymer solutions have recently been completed,[65] and other fluorescence approaches for monitoring the diffusion of nonaromatic molecules smaller than benzene in polymers near T_g are also being developed.[66]

Conclusions

A theoretical formalism, involving fluorescence NRET and Fickian diffusion of small molecule chromophores in layered polymer films, has been developed to relate quantitatively the chromophore diffusion coefficient to changes in energy transfer efficiency. Employing this formalism we have demonstrated using rubbery polymers near T_g the ability of fluorescence NRET to measure extremely low diffusion coefficients, of the order 10^{-16} cm^2/s, within reasonable experimental times, by both *in situ* steady-state intensity and *ex situ* fluorescence intensity decay measurement techniques. These measurements also confirmed the assumption of Fickian diffusion through the proportionality of energy transfer efficiency to the square root of annealing time.

Because many hundreds of NRET donor−acceptor pairs exist,[23] this approach allows for careful examination of how size, shape, and flexibility affect chromophore diffusion through a polymer matrix. Among the four chromophores studied here, significant differences in both the magnitude and the temperature dependence of D were observed. Chromophore size

played a key role in determining the magnitude of D, with a doubling of chromophore volume (pyrene vs decacyclene) resulting in an ca. 3 orders of magnitude decrease in D near the T_g of PiBMA. Other factors being equal, chromophore flexibility increases D as does an increase in aspect ratio. The temperature dependence of the diffusion data was compared to that of the polymer α-relaxation through the parameter ξ. For the two rigid molecules studied, pyrene and decacyclene, the ratios of the ξ values and the molar volumes were essentially equal, in accordance with eq 17 and consequently the Vrentas−Duda free volume theory[49] interpretation of the parameter ξ. However, this relationship does not appear to hold for the flexible molecule TC1 or the elongated BPEA molecule. For BPEA this deviation is attributed to the shape of the molecule, a characteristic which free volume theory does not take into account, resulting in greater anisotropy of diffusion than for the other chromophores. This highly anisotropic diffusion of the elongated molecule may follow a reduced temperature dependence in comparison to the less anisotropic diffusion of a disk-shaped molecule of similar molar volume.

From a comparison of the translational and rotational dynamics of the TC1 molecule in PiBMA, two anomalous effects are observed. First, there is an apparent enhancement in translational diffusion relative to rotational reorientation dynamics, with the average translational displacement of a chromophore during an average rotational relaxation time, $\langle\tau_{rot}\rangle$, being a few orders of magnitude larger than the length of the molecule. This behavior may be explained by significant local-scale heterogeneity in the polymer, as illustrated by the broad distribution of polymer α-relaxation times. For a very broad distribution of α-relaxation times, which are considered to be equivalent to rotational relaxation times for the system studied here, $\langle\tau_{rot}\rangle$ reflects only the longer relaxation times. In contrast, because translational diffusion is fastest in the most mobile regions with the shortest relaxation times, D reflects the part of the distribution with the shorter relaxation times. The second anomaly concerns the different temperature dependencies of $\langle\tau_{rot}\rangle$ and D near T_g. Heterogeneity alone is insufficient to account for this result. Instead, it may be explained qualitatively by a strong temperature dependence of the breadth of the distribution of α-relaxation times, which is known to be present in the TC1−PiBMA system employed in this comparison as well as a variety of other polymer systems near T_g. A quantitative analysis of this effect and more extensive studies of translational diffusion of small molecule chromophores, including the effects of size, shape, and flexibility, in polymers at temperatures both above and below T_g are forthcoming.

Acknowledgment. We gratefully acknowledge the National Science Foundation through the MRL program of the Materials Research Center of Northwestern University (Award DMR-9120521) and the receipt of an NSF Graduate Research Fellowship (D.D.D.) and a Terminal-Year Cabell Fellowship (A.D.) for partial support of this research. We also thank Jacob Hooker for useful discussions.

References and Notes

(1) A portion of the results of this research was originally presented at the March 1995 American Physical Society National Meeting in San Jose, CA, and at the August 1995 American Chemical Society National Meeting in Chicago, IL. See *Polym. Mater. Sci. Eng.* **1995**, *73*, 338.
(2) (a) Dhinojwala, A.; Hooker, J. C.; Torkelson, J. M. *J. Non-Cryst. Solids* **1994**, *172*−174, 286. (b) Dhinojwala, A.; Wong, G. K.; Torkelson, J. M. *J. Chem. Phys.* **1994**, *100*, 6046. (c) Dhinojwala, A.; Wong, G. K.; Torkelson, J. M. *Macromolecules* **1993**, *26*, 5943.
(3) Ehlich D.; Sillescu, H. *Macromolecules* **1990**, *23*, 1600.
(4) (a) Lu, L.; Weiss, R. G. *Macromolecules* **1994**, *27*, 219. (b) Jenkins, R.; Hammond, G. S.; Weiss, R. G. *J. Phys. Chem.* **1992**, *96*, 496. (c) He, Z.; Hammond, G. S.; Weiss, R. G. *Macromolecules* **1992**, *25*, 1568. (d) He, Z.; Hammond, G. S.; Weiss, R. G. *Macromolecules* **1992**, *25*, 501. (e) Naciri, J.; Weiss, R. G. *Macromolecules* **1989**, *22*, 3928.
(5) Vyprachticky, D.; Morawetz, H.; Fainzilberg, V. *Macromolecules* **1993**, *26*, 339.
(6) Rabe, T. E.; Tilton, R. D. *J. Colloid Interface Sci.* **1993**, *159*, 243.
(7) Smith, B. A. *Macromolecules* **1982**, *15*, 469.
(8) Byers, G. W. *Macromolecules* **1993**, *26*, 4242.
(9) Krongauz, V. V.; Yohannan, R. H. *Polymer* **1990**, *31*, 1130.
(10) Farinas, K. C.; Doh, L.; Venkatraman, S.; Potts, R. O. *Macromolecules* **1994**, *27*, 5220.
(11) Ogawa, T.; Nagata, T.; Hamada, Y. *J. Appl. Polym. Sci.* **1993**, *159*, 243.
(12) Storey, R. F.; Mauritz, K. A.; Cole, B. B. *Macromolecules* **1991**, *24*, 450.
(13) Krongauz, V. V.; Mooney, W. F.; Schmelzer, E. R. *Polymer* **1994**, *35*, 929.
(14) Arnould, D.; Laurence, R. *Ind. Eng. Chem. Res.* **1991**, *31*, 218.
(15) Hadj Romdhane, I.; Danner, R. P.; Duda, J. L. *Ind. Eng. Chem. Res.* **1995**, *34*, 2833.
(16) (a) Xia, J.; Wang, C. H. *J. Polym. Sci.: Polym. Phys. Ed.* **1995**, *33*, 899. (b) Zhang, X. Q.; Wang, C. H. *J. Polym. Sci.: Polym. Phys. Ed.* **1994**, *32*, 569. (c) Wang, C. H.; Xia, J. L.; Yu, L. *Macromolecules* **1991**, *24*, 3638. (d) Wang, C. H.; Xia, J. L. *J. Chem. Phys.* **1990**, *92*, 2603. (e) Xia, J. L.; Wang, C. H.; Li, B. Y. *Macromolecules* **1990**, *23*, 2739.
(17) Kim, H.; Waldow, D. A.; Han, C. C.; Tran-Cong, Q.; Yamamoto, M. *Polym. Commun.* **1991**, *32*, 108.
(18) Zielinski, J. M.; Heuberger, G.; Sillescu, H.; Wiesner, U.; Heuer, A.; Zhang, Y.; Spiess, H. W. *Macromolecules* **1995**, *28*, 8287.
(19) Chapman, B. R.; Paulaitis, M. E. Presentation given at the March 1995 American Physical Society National Meeting in San Jose, CA; abstract can be found in *Bull. Am. Phys. Soc.* 1995, *40* (1), 232.
(20) Cicerone, M. T.; Blackburn, F. R.; Ediger, M. D. *Macromolecules* **1995**, *28*, 8224.
(21) Rutherford backscattering spectroscopy has been employed recently to follow the non-Fickian diffusion of resorcinol bis-(diphenyl phosphate) in glassy Ultem, a poly(ether imide) (Nealey, P. F.; Cohen, R. E.; Argon, A. S. *Polymer* **1995**, *36*, 3687). Magnetic resonance imaging has also been used to monitor Fickian and non-Fickian diffusion of sorbents in polymers (Ercken, M.; Adriaensens, D.; Vanderzande, D.; Gelan, J. *Macromolecules* **1995**, *28*, 8541).
(22) Dhinojwala, A.; Torkelson, J. M. *Macromolecules* **1994**, *27*, 4817.
(23) Berlman, I. B. *Energy Transfer Parameters of Aromatic Compounds;* Academic Press: New York, 1973.
(24) (a) Karim, A.; Felcher, G. P.; Russell, T. P. *Macromolecules* **1994**, *27*, 6973. (b) Whitlow, S. J.; Wool, R. P. *Macromolecules* **1991**, *24*, 5926. (c) Green, P. F.; Kramer, E. J. *Macromolecules* **1986**, *19*, 1108. (d) Kausch, H. H.; Tirrell, M. *Annu. Rev. Mater. Sci.* **1989**, *19*, 341.
(25) Note that D is a tracer diffusion coefficient, which describes the diffusion of an infinitesimal concentration of tracer molecules through a continuous matrix. T_g's as measured by DSC for the polymers employed in this study, PiBMA and PEMA, were unchanged by the low level of labeling or doping with chromophores; therefore, the introduction of the fluorescent chromophores at low levels does not significantly affect polymer dynamics in these systems. Thus, the dopant chromophores can be considered as diffusing from one film, of infinitesimal chromophore content, to another of zero concentration. Consequently, it can be assumed that the layered films used in this study constitute a continuous matrix through which the donor molecules diffuse.
(26) Crank, J. *The Mathematics of Diffusion*; Oxford University Press: New York, 1980.
(27) Förster, T. *Ann. Phys.* **1948**, *2*, 55.
(28) Förster, T. *Molecular Spectroscopy*; Butterworths Scientific Publications: London, 1962.

(29) From ref 23, the Förster radius, R_o, for pyrene donor-to-donor energy transfer (in which pyrene acts as both donor and acceptor) is 1.0 nm. The efficiency, or probability, of energy transfer is given by $E = R_o^6/(R_o^6 + r_o^6)$, where r_o is the average separation distance between donor molecules. In a film containing a pyrene concentration of 0.12 mol %, as employed in this study, r_o can be calculated to be ca. 5.6 nm. This yields a probability for donor-to-donor energy transfer of $E = 4.1 \times 10^{-5}$, which is negligible.

(30) Prior to diffusion, there is a region at the interface of thickness approximately equal to $2R_o$ in which NRET will occur with some likelihood. Since the thinnest films used in this study are 0.38 μm and the largest R_o is 3.5 nm, this interfacial region constitutes at most a fraction of a percent of the total "sandwich" thickness. Consequently, even in the worst case studied here, <1% of the chromophores in the film sandwich are close enough before annealing to undergo any NRET.

(31) McKusick, B. C.; Heckert, R. E.; Clairns, T. L.; Coffman, D. D.; Mower, H. F. *J. Am. Chem. Soc.* **1958**, *80*, 2806.

(32) Poly(isobutyl methacrylate) and poly(ethyl methacrylate) exhibit very little change in T_g even upon the addition of several weight percent of a variety of dopants. See ref 2c and Hamilton, K. E.; Torkelson, J. M. Manuscript in preparation.

(33) Lakowicz, J. R. *Principles of Fluorescence Spectroscopy;* Plenum Press: New York, 1983.

(34) Decacyclene has very low solubility in most solvents, including chloroform. As a result, aggregates, with low absorbance and subsequently poor NRET acceptor properties, may form in solutions more concentrated than about 6×10^{-5} M. Solutions used to prepare decacyclene-doped films for this study were sufficiently dilute to prevent aggregate formation.

(35) (a) Royal, J. S.; Torkelson, J. M. *Macromolecules* **1993**, *26*, 5331. (b) Royal, J. S.; Torkelson, J. M. *Macromolecules* **1992**, *25*, 1705. (c) Royal, J. S. Ph.D. Thesis, Northwestern University, Evanston, IL, 1991.

(36) O'Connor, D. V.; Phillips, D. *Time-Correlated Single Photon Counting*; Academic Press: New York, 1984.

(37) Bennett, R. G. *J. Chem. Phys.* **1964**, *41*, 3037.

(38) It was recently noted (Farinha, J. P. S.; Martinho, J. M. G.; Yekta, A.; Winnik, M. A. *Macromolecules* **1995**, *28*, 6084) that in an experiment of the type proposed here, there is not an exactly uniform distribution of chromophores surrounding each donor, which may result in slight differences in energy transfer efficiency from that predicted by Förster theory using a totally random distribution. For diffusion coefficients approximating those obtained in this study (10^{-15} cm^2/s), these differences are potentially resolvable only in the case of very large Förster radii (6 nm) and very thin films (65 nm was the example used) at very short diffusion times (<10 min). Such effects are not resolvable within experimental error for any of the conditions employed in this study, justifying the comparison of experimental data to the prediction of the Förster theory.

(39) Berlman, I. B. *Handbook of Fluorescence Spectra of Aromatic Molecules;* Academic Press: New York, 1971.

(40) (a) Wallace, W. E.; van Zanten, J. H.; Wu, W. L. *Phys. Rev. E* **1995**, *52*, R3329. (b) Wu, W. L.; van Zanten, J. H.; Orts, W. J. *Macromolecules* **1995**, *28*, 771. (c) Keddie, J. L.; Jones, R. A. L.; Cory, R. A. *Europhys. Lett.* **1994**, *27*, 59. (d) Orts, W. J.; van Zanten, J. H.; Wu, W. L.; Satija, S. K. *Phys. Rev. Lett.* **1993**, *71*, 867. (e) Beaucage, G.; Composto, R.; Stein, R. S. *J. Polym. Sci.: Polym. Phys. Ed.* **1993**, *31*, 319.

(41) Jao, T. C.; Mishra, M. K.; Rubin, I. D.; Duhamel, J.; Winnik, M. A. *J. Polym. Sci.: Polym. Phys. Ed.* **1995**, *33*, 1173.

(42) Although pyrene-labeled polymer films produce non-single-exponential decay profiles, polymer films containing pyrene as a dopant chromophore do, in fact, yield single-exponential decay profiles. Single-exponential decays with a pyrene dopant excited-state lifetime of 291 ns have been obtained at room temperature from glassy PiBMA films as thin as 2 μm containing as little as 0.05 mol % pyrene.

(43) Dhinojwala, A. Ph.D. Thesis, Northwestern University, Evanston, IL, 1994.

(44) Hooker, J. C.; Torkelson, J. M. *Macromolecules* **1995**, *28*, 7683.

(45) Ferry, J. D. *Viscoelastic Properties of Polymers,* 3rd ed.; Wiley: New York, 1980.

(46) In the normal form of the WLF equation ($\xi = 1$), the left-hand side of eq 15 is given as $-\log(a_T)$, where a_T is a shift factor equal to $\eta(T)/\eta(T_g)$. Assuming applicability of the Stokes−Einstein equation, the quantity $D\eta/T$ is a constant, yielding $-\log[\eta(T)/\eta(T_g)] = \log\{[T_g D(T)]/[T D(T_g)]\} = \log[D(T)]/[D(T_g)]\} + \log(T_g/T)$. In diffusion experiments, D can change 1 order of magnitude over a small temperature range (absolute temperature changes of only a few percent), so the term $\log(T_g/T)$ can be neglected with little error (this is true even if the Stokes−Einstein equation is not strictly applicable as the parameter ξ accounts for the deviation from Stokes−Einstein behavior; (see references 3 and 15 where this has been done previously).

(47) Haward, R. N. *J. Macromol. Sci. - Rev. Macromol. Chem.* **1970**, *C42* (2), 191.

(48) Given the fact that two slightly different sets of WLF parameters, C_{1g} and C_{2g}, are able to fit the diffusion data with somewhat different ξ values, too much emphasis should not be placed on the exact calculated values of ξ. For example, for the diffusion of TTI in polystyrene, ref 3 lists a ξ value of 0.75, whereas ref 18 cites that $\xi = 0.84$; it may be stated that in this case $\xi \approx 0.8$. In addition the value of $\xi = 1.06$ for TTI in polyisoprene reported in ref 18 could be considered to be 1.00, within experimental error. In the present study, it may be sufficient to note that ξ is about 0.4 for pyrene in PiBMA and about 0.8−0.9 for decacyclene in PiBMA.

(49) (a) Vrentas, J. S.; Duda, J. L. *J. Appl. Polym. Sci.* **1977**, *21*, 1715. (b) Vrentas, J. S.; Liu, H. T.; Duda, J. L. *J. Appl. Polym. Sci.* **1980**, *25*, 1297. (c) Vrentas, J. S.; Duda, J. L.; Ling, H.-C. *J. Polym. Sci.: Polym. Phys. Ed.* **1985**, *23*, 275. (d) Vrentas, J. S.; Duda, J. L.; Ling, H.-C.; Hou, A. C. *J. Polym. Sci.: Polym. Phys. Ed.* **1985**, *23*, 289. (e) Vrentas, J. S.; Duda, J. L.; Hou, A. C. *J. Polym. Sci.: Polym. Phys. Ed.* **1985**, *23*, 2469. (f) Vrentas, J. S.; Duda, J. L.; Hou, A. C. *J. Appl. Polym. Sci.* **1986**, *31*, 739.

(50) (a) Chang, I.; Fujara, F.; Geil, B.; Heuberger, G.; Mangel, T.; Sillescu, H. *J. Non-Cryst. Solids* **1994**, *172*−174, 248. (b) Fujara, F.; Geil, B.; Sillescu, H.; Fleischer, G. *Z. Phys. B: Condens. Matter* **1992**, *88*, 195. (c) Kind, R.; Liechti, O.; Korner, N.; Hullinger, J.; Dolinsek, J.; Blinc, R. *Phys. Rev. B* **1992**, *45*, 7697. (d) Rössler, E. *Phys. Rev. Lett.* **1990**, *65*, 1595.

(51) Chung, S. H.; Jeffrey, K. R.; Stevens, J. R. *Phys. Rev. B* **1995**, *51*, 2826.

(52) (a) Blackburn, F. R.; Cicerone, M. T.; Hietpas, G.; Wagner, P. A.; Ediger, M. D. *J. Non-Cryst. Solids* **1994**, *172*−174, 256. (b) Blackburn, F. R.; Cicerone, M. T.; Ediger, M. D. *J. Polym. Sci.: Polym. Phys. Ed.* **1994**, *32*, 2595. (c) Note that in the studies listed in parts a and b, probe rotational reorientation measurements were made in polystyrene and compared to translational diffusion results from similarly sized, but not identical, probes in polystyrene as reported in ref 3.

(53) Hamilton, K. E.; Torkelson, J. M. Manuscript in preparation.

(54) (a) Stillinger, F. H. *Science* **1995**, *267*, 1935. (b) Mohanty, U. *Adv. Chem. Phys.* **1995**, *89*, 89. (c) Tarjus, G.; Kivelson, D. *J. Chem. Phys.* **1995**, *103*, 3071.

(55) Cicerone, M. T.; Blackburn, F. R.; Ediger, M. D. *J. Chem. Phys.* **1995**, *102*, 471 and references therein.

(56) Dhinojwala, A.; Hooker, J. C.; Torkelson, J. M. *ACS Symp. Ser.* **1995**, *601*, 318.

(57) Ngai, K. L.; Plazek, D. J. *Rubber Chem. Technol.* **1995**, *68*, 376.

(58) (a) Schmidt-Rohr, K.; Spiess, H. W. *Phys. Rev. Lett.* **1991**, *66*, 3020. (b) Schmidt-Rohr, K. *J. Non-Cryst. Solids* **1994**, *172*−174, 737.

(59) Dhinojwala, A.; Torkelson, J. M. Manuscript in preparation.

(60) Dhinojwala, A.; Deppe, D. D.; Hamilton, K. E.; Hooker, J. C.; Torkelson, J. M. Manuscript in preparation.

(61) Floudas, G.; Placke, P.; Stepanek, P.; Brown, W.; Fytas. G.; Ngai, K. L. *Macromolecules* **1995**, *28*, 6799.

(62) Dhinojwala, A.; Torkelson, J. M. Manuscript in preparation.

(63) Inoue, T.; Cicerone, M. T.; Ediger, M. D. *Macromolecules* **1995**, *28*, 3425.

(64) Deppe, D. D.; Miller, R. D.; Torkelson, J. M. *J. Polym. Sci.: Polym. Phys. Ed.*, manuscript submitted.

(65) Wisnudel, M.; Torkelson, J. M. *AIChE J.* **1996**, *42*, 1157; *Macromolecules*, manuscript submitted.

(66) Miller, K. E.; Krueger, R. H.; Torkelson, J. M. *J. Polym. Sci.: Polym. Phys. Ed.* **1995**, *33*, 2343.

(67) Differences in the T_g values for the PEMA samples used in this study and those used by Ehlich and Sillescu in ref 3 are likely due to slight differences in local tacticity associated with different polymerization temperatures, known to affect T_g in methacrylate-based polymers.

MA960024J